Supporting Information for

Reduction of carrier density and enhancement of the bulk Rashba spin-orbit coupling strength in Bi_2Te_3/GeTe superlattices

Seong Won Cho[1,2,†], Young Woong Lee[1,3], Sang Heon Kim[1,4], Seungwu Han[2], Inho Kim[1], Jong-Keuk Park[1], Joon Young Kwak[1], Jaewook Kim[1], YeonJoo Jeong[1], Gyu Weon Hwang[1], Kyeong Seok Lee[1], Seongsik Park[1], and Suyoun Lee[1,5,*]

[1]Center for Neuromorphic Engineering, Korea Institute of Science and Technology, Seoul 02792, Korea

[2]Department of Materials Science and Engineering, Seoul National University, Seoul 08826, Korea

[3]Department of Physics, Konkuk University, Seoul 05029, Korea

[4]Department of Materials and Science Engineering, Korea University, Seoul 02841, Korea

[5]Division of Nano & Information Technology, Korea University of Science and Technology, Daejeon 34316, Korea

* e-mail: slee_eels@ kist.re.kr

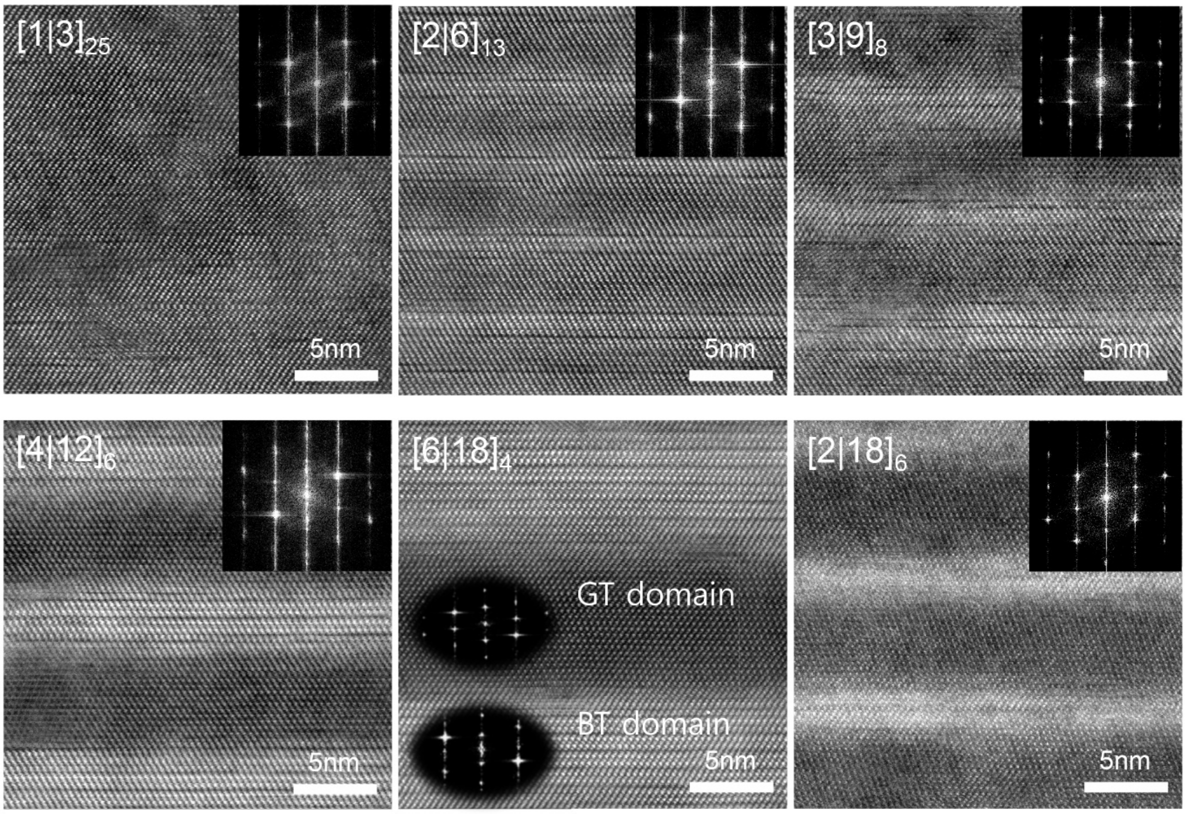

Fig. S1. The cross-section STEM images of the symmetric ($[1|3]_{25}$, $[2|6]_{13}$, $[3|9]_{8}$, $[4|12]_{6}$, and $[6|18]_{4}$) and the asymmetric ($[2|18]_{6}$) [BT|GT] SLs., where $[x|y]_z$ notation represents an SL composed of x (u.c.) of the layer BT and y (u.c.) of the GT layer with z representing the repetitions of the layers. Fast Fourier transformation of the images is shown as an inset together with each STEM image.

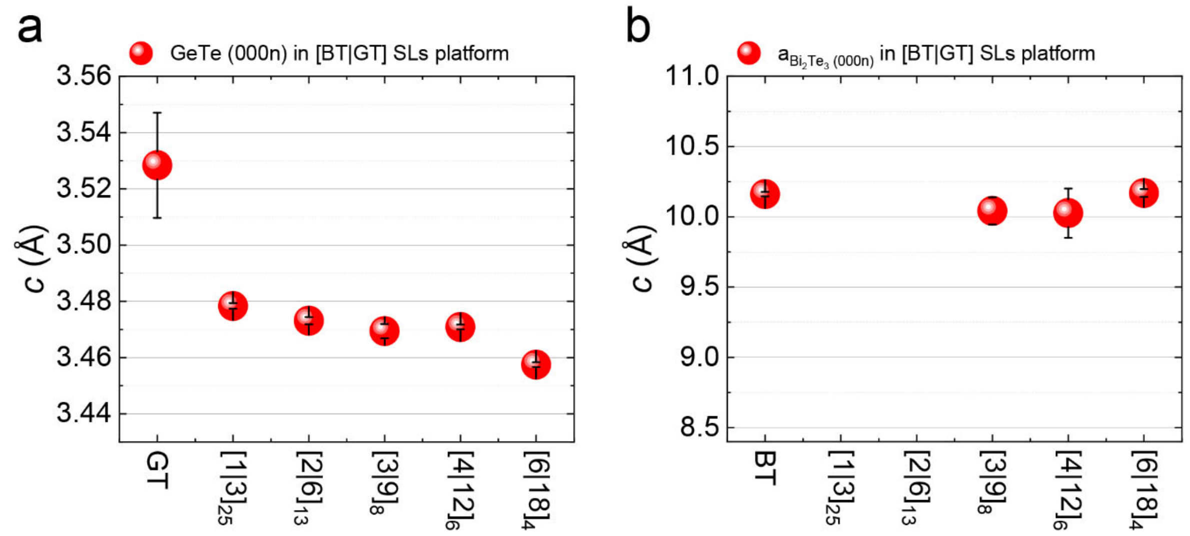

Fig. S2. The *c*-lattice constant of GT (0003) (a) and BT (0003) (b), which are calculated from the XRD peaks in Fig. 1c of the main text.

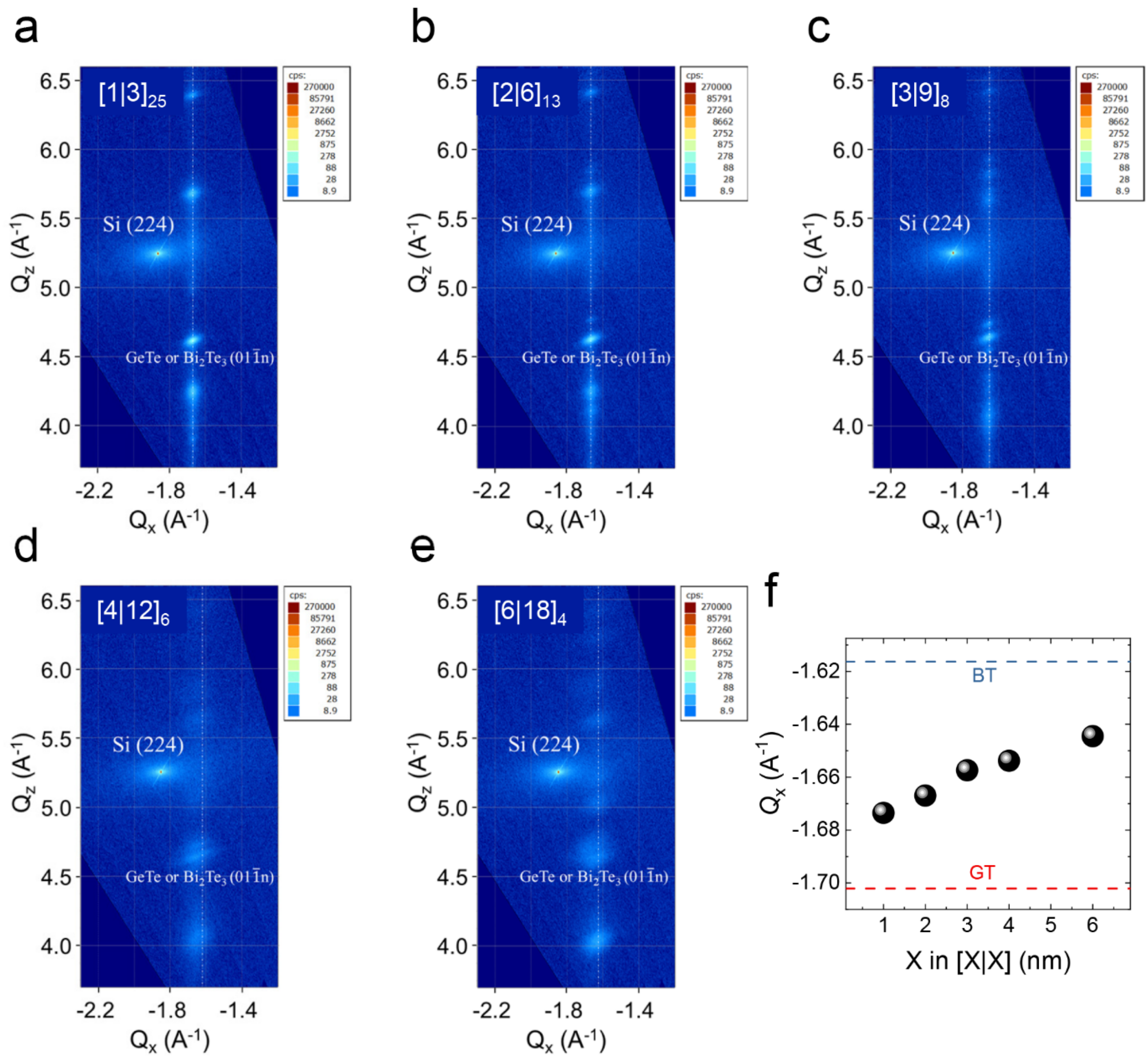

Fig. S3. (a)-(e) XRD reciprocal lattice map around Si (224) of the symmetric [BT|GT] SLs. (f) The changes of Q_x of asymmetric (0,1,-1,n) reflections according to increasing period.

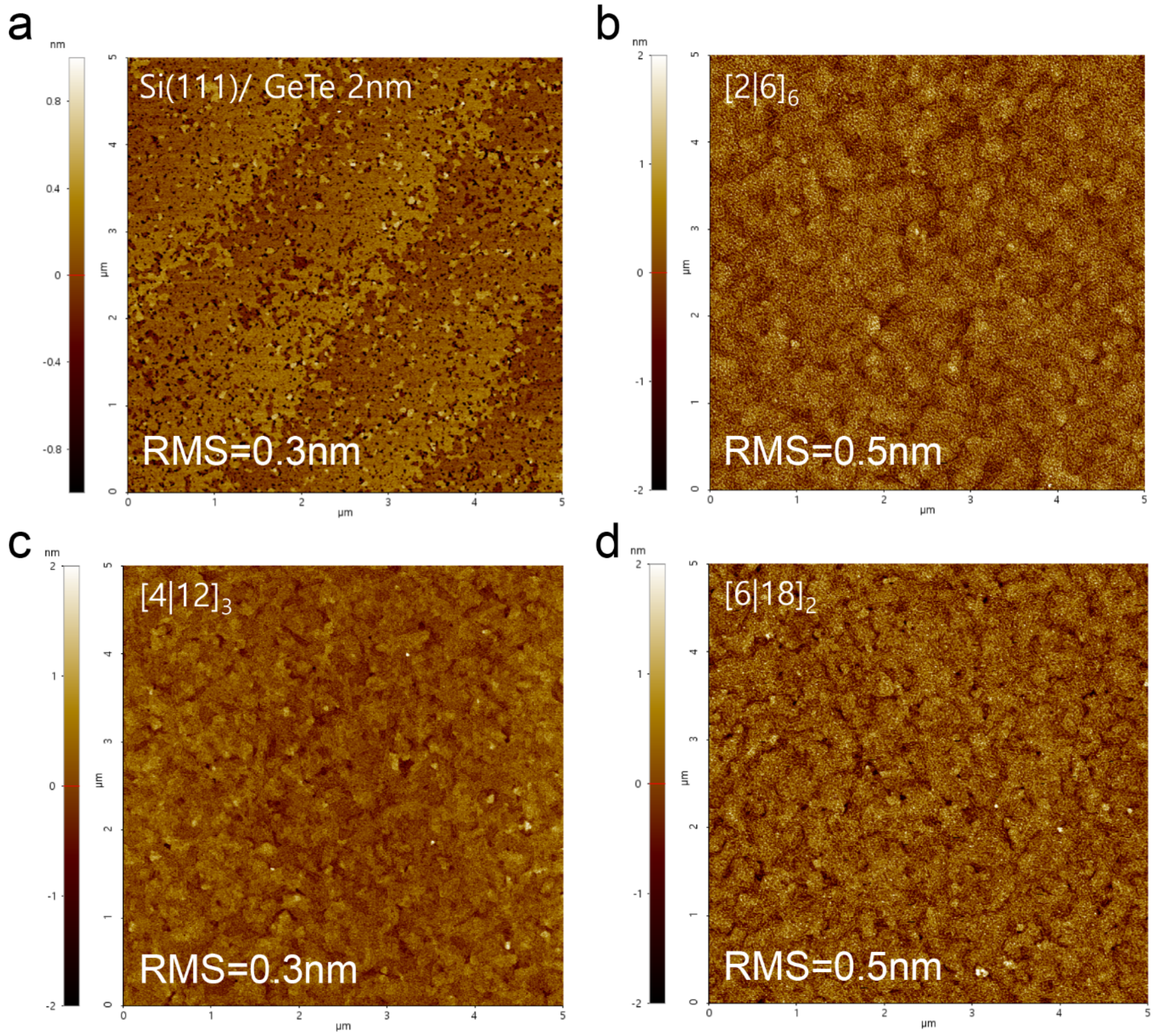

Fig. S4. AFM topography of the GeTe 2 nm template layer on Si (111) substrate (a), $[2|6]_6$ (b), $[4|12]_3$ (c), and $[6|18]_2$ (d) [BT|GT] SLs.

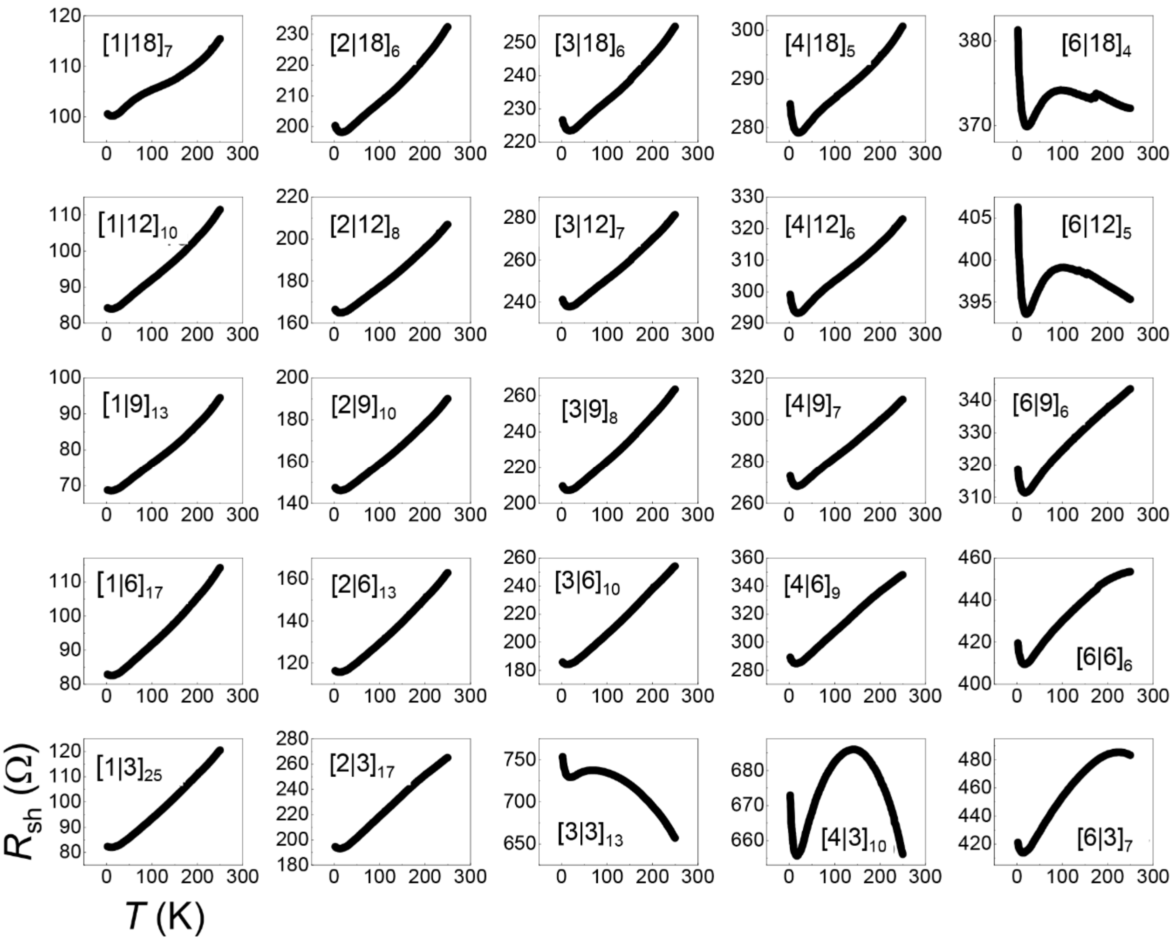

Fig. S5. The sheet resistance (R_{sh}) as a function of the temperature (T) of [BT|GT] SLs.

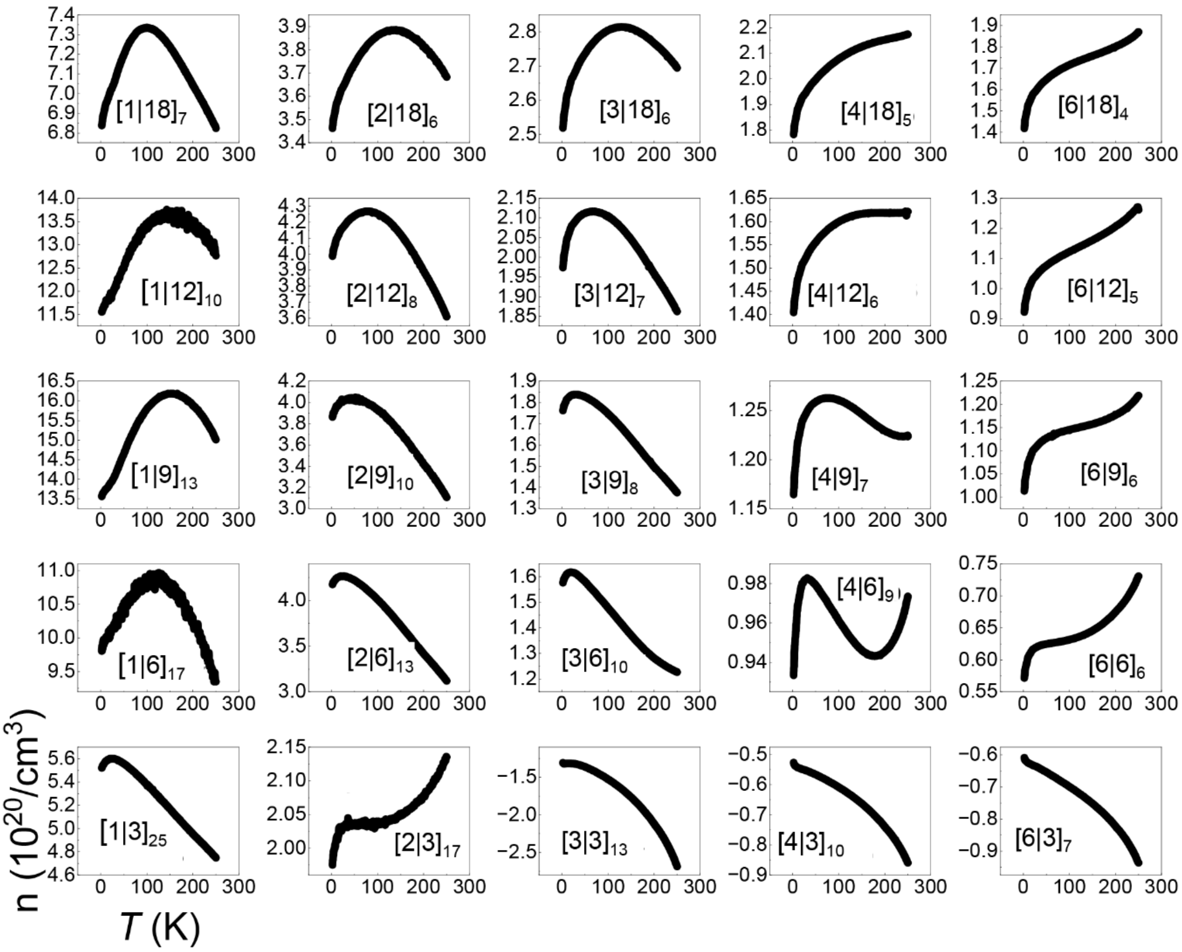

Fig. S6. The temperature-dependent carrier density (*n*) of [BT|GT] SLs. The sign of *n* means the carrier types; the positive (the negative) means hole (electron). *n* was calculated by the Hall measurement with the external magnetic field of 4 T.

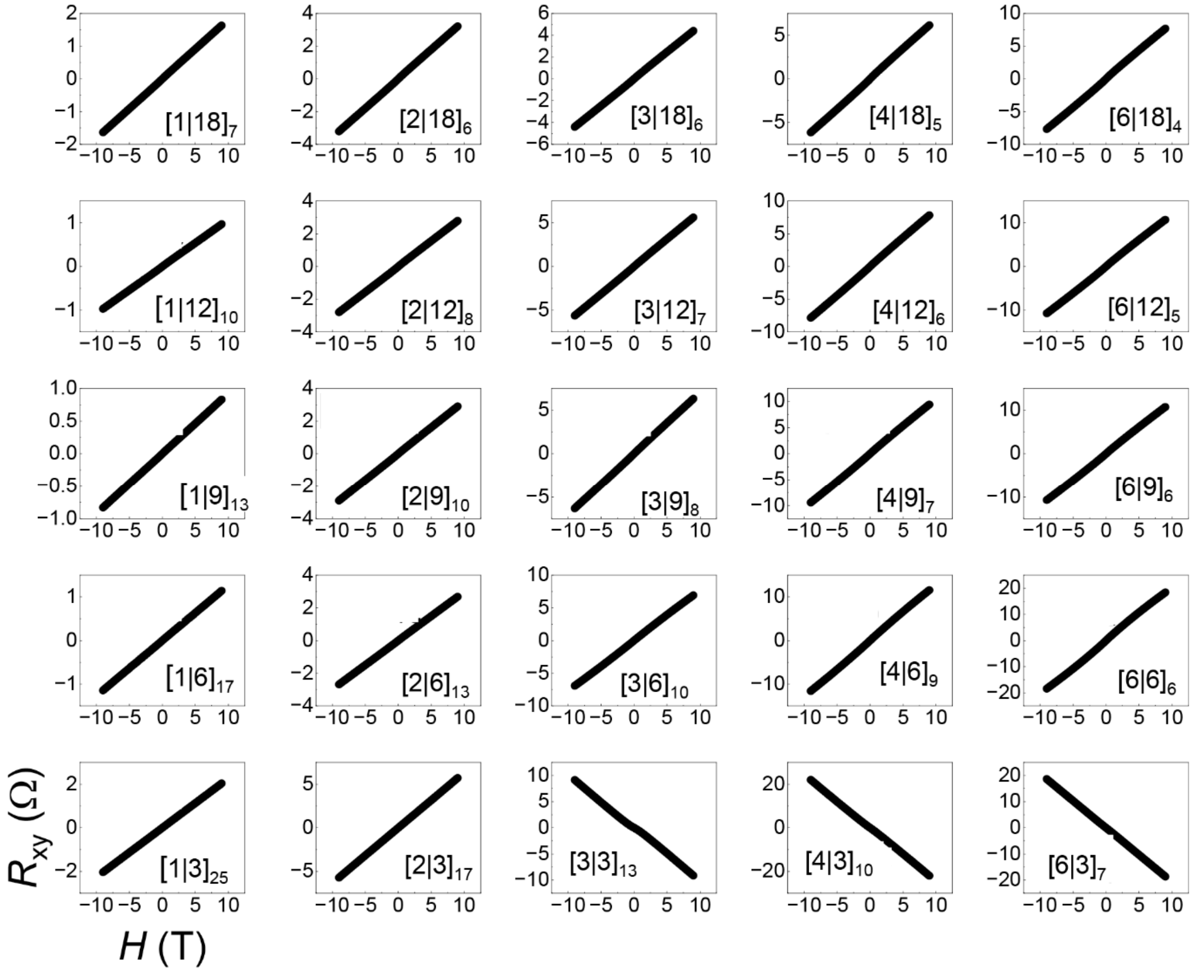

Fig. S7. The Hall resistance (R_{xy}) as a function of the magnetic field (H) of [BT|GT] SLs at T=1.8 K.

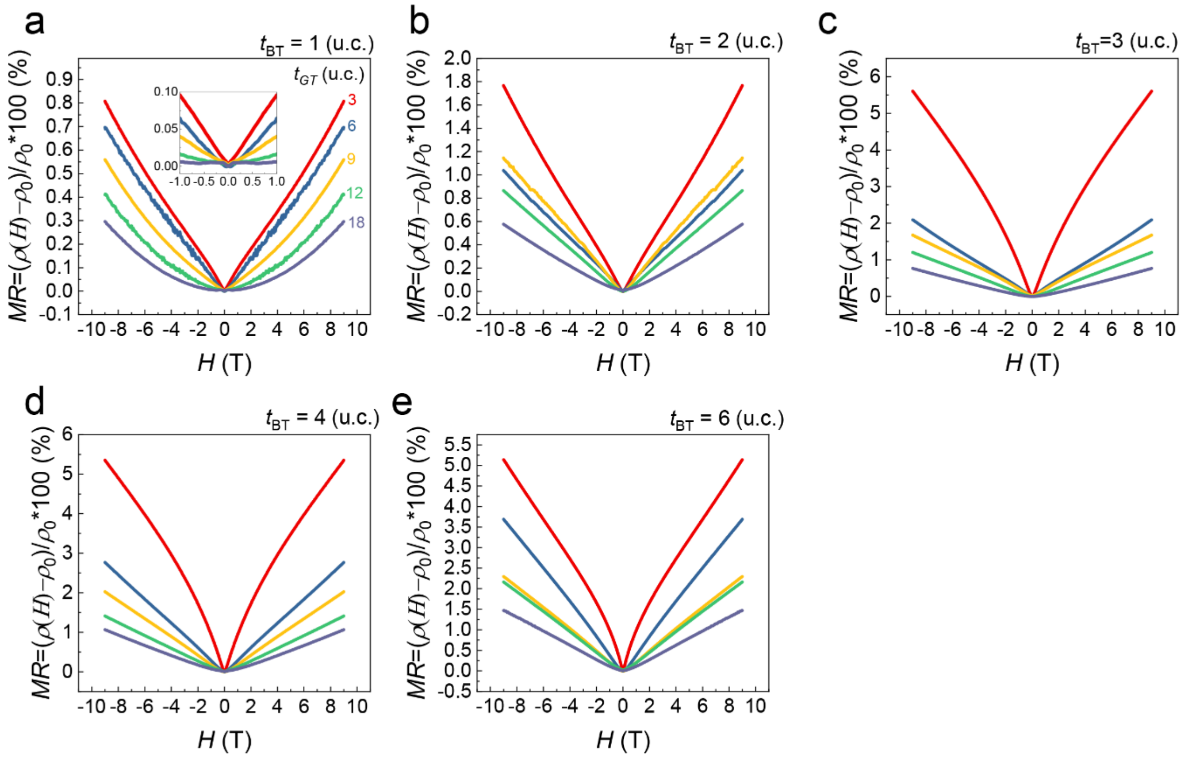

Fig. S8. The magneto-resistance (MR) of [$t_{BT}|t_{GT}$] SLs (t_{GT}=1, 2, 3, 4, and 6) as t_{BT} = 1 (a), 2 (b), 3 (c), 4 (d), and 6 (e) at T=1.8 K. The MR_{ord} is proportional to the square of mobility (μ) and magnetic field (H) ($MR_{ord} \sim (\mu H)^2$) because it is related to the scattering induced by the electron cyclone motion in a vertical magnetic field. Therefore, MR_{ord} can be expressed as $MR(H) = k(H/\rho_0)^2$ through Kohler's rule, and the constant k is a temperature invariant constant assuming that the carrier density is independent of temperature [1]. k has been extracted from $MR(H)$ of relatively high temperature (100 K) at which MR_{ord} dominates $MR(H)$, and MR_{ord} at 1.8 K has been reproduced with this k (Graphical representation of this process is shown in Fig. S10).

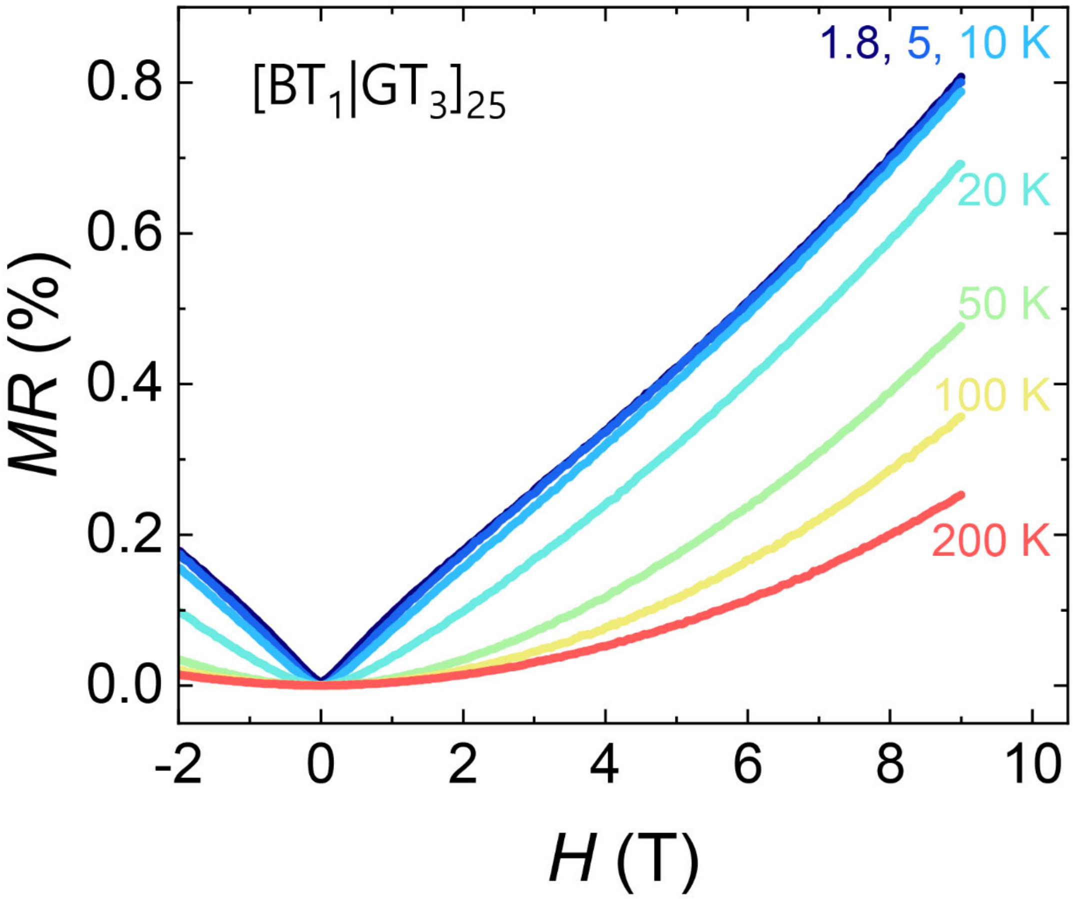

Fig. S9. Temperature dependence of the MR vs. *H* curve of an SL ($[BT_1|GT_3]_{25}$) as a representative sample

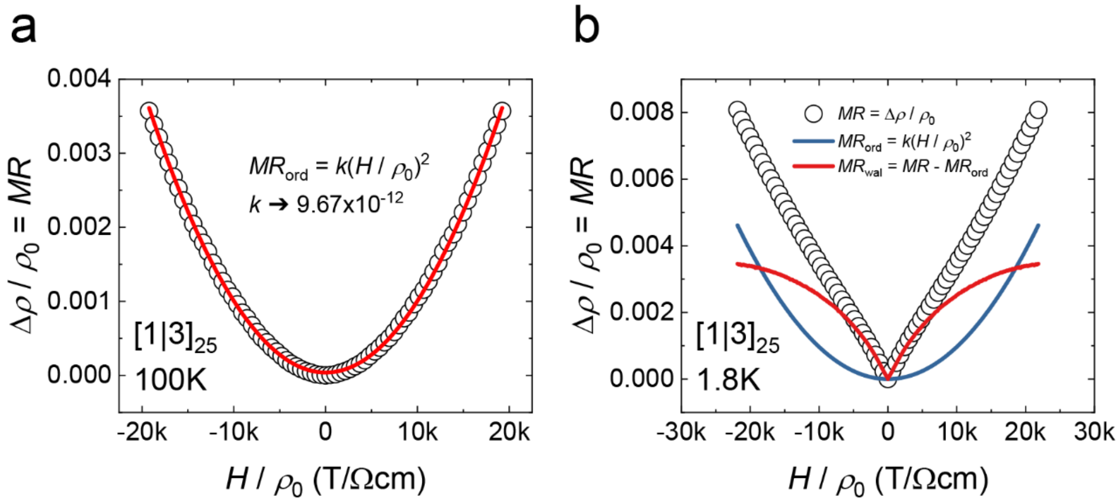

Fig. S10. Process of extraction of MR_{WAL}. (a) MR vs. H / ρ_0 curve at 100 K (black open circles), which can be fully expressed by the classical MR (MR_{ord}) with the form of $k(H/\rho_0)^2$ (red line). With k extracted from (a), the MR_{ord} at 1.8 K can be reproduced (blue line in (b)). And, the MR_{WAL} (red line in (b)) can be obtained by subtracting the MR_{ord} from raw MR (black open circles in (b)).

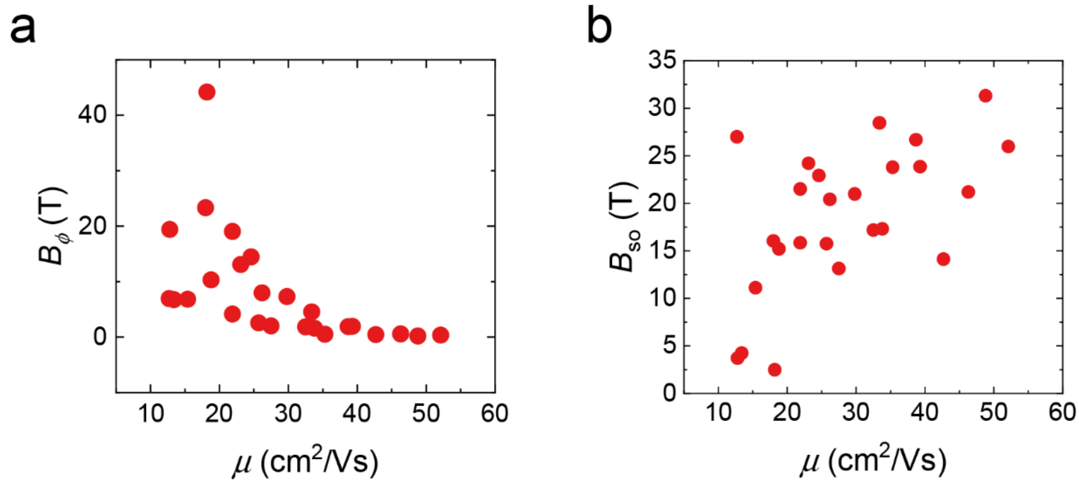

Fig. S11. The fitting parameters of B_ϕ (a) and B_{so} (b) as a function of carrier mobility.

Reference

[1] Y. Nakazawa, M. Uchida, S. Nishihaya, M. Ohno, S. Sato, and M. Kawasaki, Physical Review B **103** (2021).